HHS Public Access

Author manuscript

Acta Biomater. Author manuscript; available in PMC 2018 June 01.

Published in final edited form as:

Acta Biomater. 2017 June ; 55: 144–152. doi:10.1016/j.actbio.2017.03.050.

Distributed Vasculogenesis from Modular Agarose-Hydroxyapatite-Fibrinogen Microbeads

Ana Y. Rioja[*], **Ethan L. H. Daley**[*], **Julia C. Habif**, **Andrew J. Putnam**, and **Jan P. Stegemann**

Department of Biomedical Engineering, University of Michigan, Ann Arbor, MI, 48105

Abstract

Critical limb ischemia impairs circulation to the extremities, causing pain, disrupted wound healing, and potential tissue necrosis. Therapeutic angiogenesis seeks to repair the damaged microvasculature directly to restore blood flow. In this study, we developed modular, micro-scale constructs designed to possess robust handling qualities, allow *in vitro* pre-culture, and promote microvasculature formation. The microbead matrix consisted of an agarose (AG) base to prevent aggregation, combined with cell-adhesive components of fibrinogen (FGN) and/or hydroxyapatite (HA). Microbeads encapsulating a co-culture of human umbilical vein endothelial cells (HUVEC) and fibroblasts were prepared and characterized. Microbeads were generally 80–100 microns in diameter, and the size increased with the addition of FGN and HA. Addition of HA increased the yield of microbeads, as well as the homogeneity of distribution of FGN within the matrix. Cell viability was high in all microbead types. When cell-seeded microbeads were embedded in fibrin hydrogels, HUVEC sprouting and inosculation between neighboring microbeads were observed over seven days. Pre-culture of microbeads for an additional seven days prior to embedding in fibrin resulted in significantly greater HUVEC network length in AG+HA+FGN microbeads, as compared to AG, AG+HA or AG+FGN microbeads. Importantly, composite microbeads resulted in more even and widespread endothelial network formation, relative to control microbeads consisting of pure fibrin. These results demonstrate that AG+HA+FGN microbeads support HUVEC sprouting both within and between adjacent microbeads, and can promote distributed vascularization of an external matrix. Such modular microtissues may have utility in treating ischemic tissue by rapidly re-establishing a microvascular network.

Graphical abstract

Address: Jan P. Stegemann, Ph.D., University of Michigan, Department of Biomedical Engineering, 2146 Lurie Biomedical Engineering Building, 1101 Beal Ave. Ann Arbor, MI 48109, Tel: 734-764-8313, Fax: 734-647-4834, jpsteg@umich.edu.

[*]Co-first authors

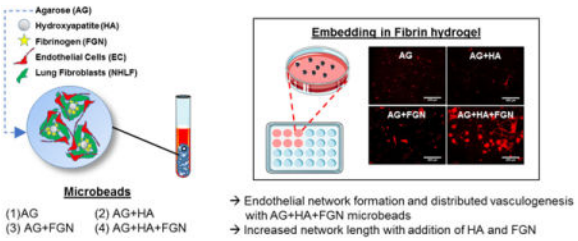

1. Introduction

Peripheral arterial disease (PAD) is caused by the obstruction/reduction of blood flow in the arteries due to atherosclerotic plaque formation. As PAD progresses, patients begin to experience pain in the limbs even at rest. This chronic and final stage of PAD, critical limb ischemia (CLI), can result in the loss of the affected limb due to ulceration or gangrene [1, 2]. Though CLI patients represent only 1% of all PAD sufferers, this condition is associated with significant rates of mortality (nearly 50% after 5 years) as well as a substantial economic burden [2].

CLI treatment involves restoration of blood flow to the extremities to prevent tissue necropathy and eventual amputation. While pharmaceutical options such as statin therapy are available to treat CLI [3], surgical interventions are sometimes employed if the patient is healthy enough for surgery. However, patients with medical co-morbidities may be poor candidates for highly invasive surgical procedures [2]. For these patients, it is advantageous to treat the ischemic tissue directly by repairing the microvasculature in a minimally invasive manner. Treating CLI in a more localized fashion may reduce ulceration and improve outcomes in diabetic patients.

Currently there is no specific treatment for the repair of damaged microvasculature that causes ulceration in CLI. However, by combining cells, growth factors and biomaterial scaffolds, a tissue engineering strategy offers a compelling and potentially minimally invasive means of promoting the repair of microvasculature in ischemic tissues. A variety of materials, cells, and growth factors have been employed to treat ulcers [4–6]. Modular tissue engineering offers a refinement of the tissue engineering strategy in which small scaffold “building blocks” can be generated and assembled into larger engineered constructs [7]. The use of engineered microtissues has been shown to reduce the oxygen and nutrient diffusion limitations that hamper larger constructs [8–13]. Moreover, microtissues can be designed to be delivered in a minimally invasive manner or assembled into macrostructures.

A key consideration when developing engineered vascular microtissues is enabling the establishment of vascularization in vitro prior to implantation. After implantation in an ischemic site, pre-vascularized microtissues could accelerate the restoration of the microvasculature by jump-starting anastomosis with blood vessels in the surrounding healthy tissue. In addition, pre-vascularization may also improve the survival of the cells within the construct. A variety of materials and cell populations can be employed to engineer microtissues, depending on the application [14–21]. For revascularization strategies, pure fibrin and composites made from fibrin, agarose, collagen, and gelatin have

been used to develop engineered tissues capable of supporting endothelial vessel formation [22–25].

Past work by our group has shown that cell-encapsulating fibrin and collagen-fibrin microtissues can foster endothelial sprout formation and inosculation in a three-dimensional (3D) in vitro model [25, 26]. In particular, we have used co-cultures of endothelial cells and stromal cells to promote vessel formation in engineered tissues. Paracrine signals provided by fibroblasts or other stromal cells are important in the formation and stabilization of endothelial cell networks [23, 27–33]. In vitro studies have shown that endothelial sprout length is dependent on a variety of conditions, including extracellular matrix properties and stromal cell type [23, 25, 34].

In the present study, we build upon our previous work by developing microtissues designed to promote widespread vascular network formation, using a defined combination of naturally-derived, biomimetic biomaterials. Agarose is a relatively inert polysaccharide used in a variety of tissue engineering applications for structural support [21, 35]. It does not permit cell attachment, and therefore is often used in combination with other materials that facilitate cell adhesion and proliferation [36–38]. Hydroxyapatite (HA) is a main component of mineralized biological tissues that has been shown to adsorb and retain proteins [39–41], and may also promote vasculogenesis [42–44]. Fibrinogen (FGN) is a circulating precursor of the blood clotting protein fibrin, which is known to bind growth factors and proteins through its heparin-binding domain [45]. Incorporation of HA and FGN into agarose microtissues therefore provides a mechanically robust environment with the ability to sequester proteins and provide sites for cell attachment. Our goal was to combine these materials to create novel “microbeads” that exhibit: 1) higher production yield through a reduction in adhesion and aggregation, 2) improved injectability through reduced size and increased sphericity, and 3) more widespread vascular network formation via inosculation between sprouts from neighboring microbeads.

2. Materials and Methods

2.1 Cell culture

Human umbilical vein endothelial cells (HUVEC) from two different sources were used in these studies. For microbead characterization experiments, HUVEC were isolated from umbilical cords obtained via an IRB-exempt process from the University of Michigan Mott Children’s Hospital using previously described methodology [34]. Umbilical cords were rinsed with phosphate buffer saline (PBS) prior to digestion. Collagenase type I solution (195 U/mL, Worthington Biochemical, Lakewood, NJ) was utilized to digest cords for 20 minutes at 37 °C. Digested tissues were rinsed with PBS and centrifuged at 200 g for 5 minutes. HUVEC were plated in T25 flasks with endothelial growth media (EGM-2, Lonza). Flasks were rinsed with PBS three times, the next day, prior to media change. Additional media changes were done every 2 days. HUVEC from a commercial source (Lonza Inc, Walkersville, MD), were utilized for network length studies. We employed two different HUVEC sources to ensure the robustness of the observed phenomena independent of endothelial cell source. All experiments employed HUVEC from passages 4–7.

Normal human lung fibroblasts (NHLF, Lonza Inc., Walkersville, MD) from passages 9–14 were cultured in Media 199 (M199, Life Technologies, Grand Island, NY) with 10% fetal bovine serum (FBS). Culture media of HUVEC and NHLF were replaced every other day prior to experimental processing. EGM-2 is composed of 500 mL of endothelial basal medium, 10 mL of FBS (2% concentration), 0.5 mL of vascular endothelial growth factor (VEGF), 0.5 mL of gentamicin, amphotericin-B (GA-1000), 0.2 mL of human fibroblastic growth factor (hFGF-B), 0.5 mL of R^3-IGF-1, 0.5 mL of ascorbic acid, 0.5 mL hydrocortisone, 0.5 mL of human epidermal growth factor (hEGF), and 2.0 mL of heparin. Component' concentrations are not provided by Lonza, Inc.

2.2 Production of agarose-based microbeads

Cell-encapsulating, agarose-based microbeads were produced using a water-in-oil emulsification process (Fig 1) [46]. Emulsification was carried out in autoclaved 100 cSt polydimethylsiloxane (PDMS) oil (Clearco Products Co. Inc. Bensalem, PA).

In preparation for microbead production, HUVEC and NHLF were detached using 0.05% Trypsin-EDTA (Gibco), re-suspended in endothelial growth media (EGM-2), and counted using an automated cell counter (Multisizer 3, Beckman Coulter, Brea, CA). Fibrinogen (Sigma Aldrich, St. Louis MO) was dissolved in serum-free endothelial growth media (SFEGM-2) at 37 °C (4.0 mg/mL active clottable protein concentration), sterile filtered and kept on ice until ready for use. Agarose was warmed to 65 °C.

Microbeads components included HUVEC and NHLF (1×10^6 of cell type per mL of aqueous components), agarose (8.0 mg/mL final concentration), fetal bovine serum (FBS), hydroxyapatite (HA), and fibrinogen (FGN). The components were loaded into a 10 mL syringe and injected into the PDMS through a 25-gauge needle. A two-paddle impeller stirred the mixture at 700 rpm for 6 min at 37 °C and then for 30 min on ice to gel the resulting microbeads. Previous work has shown that use of FBS acts as a surfactant that facilitates the separation of the beads from the oil phase during production, and also aids in maintaining high cell viability [17, 21].

After mixing, the microbeads were separated from the PDMS using three centrifugation and PBS wash steps. The microbeads were then re-suspended in EGM-2 and cultured in 15 mL vented conical tubes (CELLTREAT Scientific Products, Shirley, MA). Media of constructs was changed the day after preparation and every other day after.

2.3 Embedding of microbeads in fibrin (FIB) hydrogels

Microbeads were embedded in fibrin hydrogels similarly to what was previously done [25]. The 15 mL vented conical tubes containing the media-microbead solution were centrifuged prior to the separation of the supernatant from the microbeads. All tubes were aliquoted the same way to keep comparison between batches consistent. 255 μL of microbeads were transferred from the culture tubes and placed into new tubes. 100 μL of FBS (10% final), 20 μL of 50 U/mL thrombin (1 U/mL final), and 625 μL of fibrinogen stock (2.5 mg/mL final clottable protein concentration) were added atop of the microbeads and mixed thoroughly to make 2 fibrin hydrogels with microbeads. 500 uL of the total solution was added to each well of a 24-well plate and left in the incubator for approximately 30 minutes to allow

complete gelation of the fibrin hydrogels. 1 mL of media was added to each hydrogel after the gelation process. Media was replaced the next day and every other day until the experimental end points.

2.4 Microbead characterization

Prior to microbead size quantification, images of microbeads were taken using Nikon DS-Ri2 camera. The rectangular selection tool in ImageJ (National Institutes of Health, Bethesda, MD) was utilized to measure microbead size. The average horizontal and vertical diameter of the first 25 microbeads per image (100 microbeads total) were quantified to determine the average microbead diameter of each batch.

To calculate microbead yield, microbeads were counted using a hemocytometer in the same manner cell counting is done. Ten independent counts were done per microbead batch. A single-blind study was used for both microbead size and yield quantification.

2.5 Viability of encapsulated cells

Cell viability was quantified using a fluorescent live/dead assay (Thermo Fisher) as per the manufacturer's protocols. Images were captured using a fluorescent source 465-495/515-555 nm excitation/emission (calcein-AM, live cells) and 540/605 nm (ethidium bromide, dead cells) filter sets (Nikon Instruments Inc., Melville, NJ). Cells were counted using ImageJ analysis software and a custom macro (US National Institutes of Health, Bethesda, MD). Cells staining positive for calcein-AM and negative for ethidium bromide were considered live at the beginning of the assay.

2.6 Staining and visualization of microbead protein content

A non-specific protein-binding dye (EZBlue, Sigma-Aldrich) was used to visualize protein content. Microbeads were washed in PBS, and fixed overnight in buffered zinc formalin (Z-Fix, Anatech Ltd, Battle Creek, MI). Microbeads were then stained for 10 min at room temperature.

2.7 HUVEC sprout staining and quantification

Z-fix was employed to fix constructs 7 days after microbeads were embedded in fibrin hydrogels. Samples were rinsed two times before and after fixation. Ulex Europaeus Agglutinin I (UEA-I, Vector Laboratories, Burlingame, CA), an endothelial cell-specific marker, was utilized to stain the endothelial cells. Samples were stained with a 1% BSA buffer in PBS containing 10 nM DAPI and 20 μg/mL rhodamine-labeled UEA-I. After the 45 min room temperature incubation, samples were washed 2–4 times with PBS.

Prior to imaging, samples were taken out from the 24-well tissue culture plates and placed on slides. Coverslips were added on top prior to imaging. An optical microscope (Olympus IX81, Olympus, Center Valley, PA) and the scan slide tool in the Metamorph software were employed to take fluorescent images of endothelial networks formed in HUVEC-NHLF microbeads that had been embedded in FIB hydrogels. The angiogenesis analyzer tool [47] and the ImageJ software were employed to measure total network length in each fibrin hydrogel. The background, brightness, contrast, and threshold of each hydrogel scan was

adjusted preceding analysis. The correct scale and possible outlier parameters were also defined before running the angiogenesis analyzer. The aforementioned processing settings were kept constant for each hydrogel scan.

2.8 Statistical Analysis

Statistical analyses were performed running a one-way ANOVA with Dunnett's T3 post hoc test using SPSS software (IBM, Armonk, NY). Experiments were repeated at least twice and each contain at least three replicates for each group. Data are reported as mean ± standard deviation. Values of $p \leq 0.05$ were considered statistically significant.

3. Results and Discussion

3.1 Microbead formulation and production

The goal of this study was to develop modular tissue engineering constructs that could be easily handled and promote vascular network formation over a broad area. Our strategy centered on agarose (AG)-based microbeads encapsulating a co-culture of endothelial cells and fibroblasts, because these cell types have been shown to form robust vascular networks in other applications. Agarose was chosen to form the bulk of the microbead volume because of its ability to produce stable, spherical microbeads while limiting the adherence of the microbeads to each other and to the surface of the cultureware used in processing and handling. Hydroxyapatite (HA) and fibrinogen (FGN) were added to the microbead formulations at defined levels to encourage cell adherence and spreading, and to promote cell-specific functions that can enhance vasculogenesis.

Water-in-oil emulsification and an alternating heating/cooling cycle consistently resulted in spherical AG-based microbeads with mean diameters ranging from 80 to 110 μm, as shown in Figure 2. Pure 8.0 mg/mL AG microbeads (Fig. 2A) were clear, colorless, and highly spherical. Addition of HA and FGN to these AG-based microbeads resulted in incorporation of the active matrix components to differing degrees. HA alone dispersed evenly throughout the microbead (Fig. 2B), whereas FGN alone was not well incorporated (Fig. 2C) and remained in the supernatant when microbeads were collected. However, addition of both HA and FGN resulted in the formation of dense and homogenously distributed HA/FGN complexes (Fig. 2D–E). These data suggest that HA serves to bind and incorporate FGN into the microbeads. The HA surface lattice contains Ca^{2+} and PO^{3-} ions that promote the adsorption of a wide range of proteins with positively or negatively charged moieties [48]. In the context of vasculogenic microbeads, the use of HA was intended to improve the incorporation of FGN into the microbeads during production and to provide a substrate for serum proteins that could further enhance cell attachment and sprout formation. Fabrication of microbeads using only 4.0 mg/mL agarose resulted in fragile microbeads and poor encapsulation of HA and FGN (Fig. 2F).

Addition of HA and FGN resulted in significantly larger microbeads compared to pure AG or AG+HA microbeads (Fig. 2G). However, there was no significant difference in diameters between microbeads containing AG+HA+0.25 mg/mL FGN and those containing AG+HA +1.25FGN. While average microbead diameters depended on the proportion of constituent

materials, the resulting microbeads were consistent with a relatively narrow size distribution, as indicated by the error bars in Fig. 2G. In all cases, the microbeads were <120 μm in diameter, such that any encapsulated cell would be less than 60 μm from the perimeter. This small diffusion distance is an advantage of the microbead format because it ensures availability of nutrients and oxygen to embedded cells.

3.2 Microbead characterization

Protein staining was used to visualize the distribution of the active matrix components and cells encapsulated within AG-based microbeads, as shown in Figure 3. Pure AG microbeads (Fig. 3A) entrapped cells efficiently, but there was no evidence of cell spreading by Day 1 in HUVEC-NHLF co-culture. Microbeads made with added FGN alone showed little incorporation of protein or cell spreading, though in the higher concentration some protein strands were evident (Fig. 3B, C). Addition of HA alone (Fig. 3D) to the microbeads indicated some entrapment of protein, presumably from the surrounding culture medium. However, addition of HA+FGN (Fig. 3E, F) resulted in very clear and widespread incorporation of protein into the microbeads, with concomitant evidence of cell adhesion and spreading. FGN is a soluble plasma protein that contains RGD domains that permit direct binding of cells [49], and its relatively high solubility enables its incorporation in the microbead fabrication process. Our results further support the idea that the incorporation of HA serves to sequester FGN, which in turn promotes cell attachment and function.

Pure fibrin (FIB) microbeads were also produced and cultured in the same manner as AG-based microbeads. However, under these conditions FIB microbeads tended to agglomerate into masses several hundred microns in diameter in culture (Fig. 3G). In contrast, AG-based microbeads remained as discrete spherical units, and did not change appreciably in size or shape. Reduced aggregation allows microbeads to be cultured in vitro over time before being injected as a slurry. Such in vitro culture periods allow the phenotype of the embedded cells to be more carefully controlled, and therefore may lead to more effective function when implanted.

Cell viability in all microbead formulations was high (Fig. 4A). Viability of HUVEC and NHLF was generally >80% in all microbead types, with no statistical differences between formulations or time in culture over a one week period. These results show that the encapsulation process itself is not harmful to cells, and that cells can maintain their viability when being cultured in microbeads. The clear survival of cells over a week in culture suggests that mass transfer limitations are not a barrier, and it is expected that cells could therefore also survive for longer periods.

Microbead composition affected the number and volume of microbeads yielded by the production process (Fig. 4B). The numerical yield of AG-only microbeads was approximately 4×10^5/mL, while the addition of HA alone increased the yield to over 7×10^5/mL. It is likely that the relatively high specific gravity of HA (3.08) reduced the buoyancy of HA-containing microbeads and thereby contributed to improved separation during centrifugation [50]. Incorporation of FGN alone decreased the microbead yield, while including HA+FGN caused a recovery in numerical yield, though not to the level of the pure AG microbeads. To further assess the effects of the active matrix components on microbead

yield, AG-based microbeads were made with HA and from 0.25 to 1.25 mg/mL FGN (Fig. 4C). Numerical yield dropped significantly when the FGN content was increased from 0.25 to 0.75 mg/mL. However, further increases in FGN concentration did not significantly affect yield. It should be noted that while large differences were observed in the numerical yields between microbead formulations, the difference in the volume of microbeads collected was not as great. This discrepancy is due to the differences in microbead size (Fig. 2G), and estimation of the microbead volume showed no significant differences between the yields of AG-only and AG+HA+0.25 mg/mL FGN microbeads (Fig. 4D).

3.3 HUVEC sprouting and network formation

Figure 5 shows images of AG+HA+0.25 mg/mL FGN with encapsulated HUVEC and NHLF in culture. These experiments were performed to verify whether endothelial cells can form sprouts within and from these microbeads, as a precursor to examining more global network formation. When microbeads were embedded in a bulk 3D fibrin hydrogel (Fig. 5A), it was evident that HUVEC could sprout from microbeads into the surrounding matrix over a week in culture, and nascent vessel networks were observed. Culture of microbeads within bulk fibrin hydrogels is used to recreate a 3D matrix to mimic the in vivo tissue environment, and similar systems have been employed to study angiogenesis and vasculogenesis [39, 52, 54]. When microbeads were cultured as discrete units without being embedded in a surrounding hydrogel (Fig. 5B), small vessel fragments formed within the microbeads. When such microbeads were pre-cultured for a week as discrete modules before being embedded in a surrounding fibrin bulk hydrogel (Fig. 5C), the vessel fragments formed within the microbeads could sprout into the surrounding matrix. Taken together, these experiments therefore established that HUVEC can form nascent vessels within AG +HA+FGN microbeads, and can sprout from the microbeads when embedded in a surrounding matrix.

The composition of the microbeads affected their ability to create distributed (i.e. spanning a large area) vessel networks, as shown in Figure 6. In these studies, microbeads were embedded in surrounding fibrin hydrogels one day after microbead production, and were then cultured for seven days. In microbeads without HA (Fig. 6A–C), sprouting was minimal and relatively local in the direct vicinity of the microbeads. Microbeads with HA but no FGN (Fig. 6D) also showed minimal and local sprouting. For microbeads that contained both HA and FGN (Fig. 6E, F), the extent of sprouting was much greater and spanned the entire volume of the surrounding fibrin matrix. In contrast, pure FIB microbeads that were cultured under similar conditions (Fig. 6G), exhibited robust but highly focal sprouting (Fig. 6G) due to aggregation of the microbeads. The limited aggregation of the AG-based microbeads led to greater homogeneity in the distribution of endothelial networks within the surrounding matrix. This effect is a potentially important feature of AG+HA +FGN microbeads, since upon implantation a more distributed vessel network could increase the probability and rate of inosculation with the host and subsequent revascularization of tissue.

The distribution of fibroblasts and endothelial cells in all four microbead conditions was assess by staining of cells 7 days after being embedded in fibrin hydrogels, as shown in

Supplementary Figure 1. All four microbead conditions formed endothelial sprouts (as previously shown); however, there were more fibroblasts and a higher number of microbeads with endothelial sprouts in the AG+1.25FGN and the AG+7.5HA+1.25FGN conditions. Fibroblasts migrated from the microbeads into the fibrin hydrogels in all conditions. A more homogeneous distribution of fibroblasts and endothelial cells was observed in the AG +7.5HA+1.25FGN condition.

The effect of pre-culture on endothelial network formation was also assessed using selected microbead formulations, as shown in Figure 7. In these experiments, a lower (7.5 mg/mL) concentration of HA was used to reduce background fluorescence and allow quantification of vessel network length. Microbeads that were embedded in 3D fibrin hydrogels one day after production (Fig. 7A–D) showed again that only local and very modest sprouting occurs into surrounding matrix, unless both HA and FGN are incorporated. In the latter case, endothelial sprouting is robust and distributed throughout the matrix. When microbeads were pre-cultured for seven days prior to being embedded in fibrin (Fig. 7E–H), the degree of sprouting was decreased in both pure AG and AG+HA samples, but was retained in the FGN and HA+FGN microbeads. Quantification of total sprout network length (Fig. 8) confirmed these observations. These data show that addition of HA+FGN caused a marked increase in total network length, relative to the other formulations. In addition, pre-culture of the AG+HA+FGN microbeads prior to embedding had a modest positive effect on network length, compared to AG+HA+FGN microbeads that had not been pre-cultured.

The fate of microbeads and the embedded cells after implantation in vivo will depend on the matrix formulation. The materials examined in this study assisted with achieving distributed vascularization, and they can be further optimized to provide desired rates of cell delivery and concomitant matrix degradation. Agarose is resistant to proteolytic degradation, but can be broken down hydrolytically over time, and is susceptible to some lysosomal enzymes. It is therefore likely to be broken down slowly in vivo, and can impart stability to the microbeads while promoting cell function. Future work will examine the remodeling and degradation of microbeads after implantation, and will also investigate other materials that can mimic the distributive effects of agarose while offering more control over degradation rate. The tailoring of matrix material properties can be used to control the distribution of vessel networks, and potentially to thereby promote more rapid and efficient inosculation with host tissue after implantation.

4. Conclusions

AG+HA+FGN microbeads supported endothelial sprouting and promoted homogeneous and widespread distribution of endothelial network formation via inosculation of endothelial sprouts between adjacent microbeads when embedded in fibrin hydrogels. The use of AG in the matrix prevented aggregation and contributed to the formation of spherical microbeads, which facilitated the culture, collection, and injection of microbead populations. The incorporation of HA and FGN within the microbeads permitted cell adhesion and spreading within the otherwise non-adherent AG. By developing these AG+HA+FGN microbeads, we have increased microbead production yield, improved injectability, and achieved a more

homogeneous vascular network. In addition, pre-culture of microbeads led to an increase in endothelial network length, which could be beneficial in ischemic applications.

Supplementary Material

Refer to Web version on PubMed Central for supplementary material.

Acknowledgments

Research reported in this publication was supported in part by the National Heart, Lung, and Blood Institute under award numbers R01HL118259 (to AJP and JPS) and by the National Institute of Arthritis and Musculoskeletal and Skin Diseases under award number R01AR062636 (to JPS). The content is solely the responsibility of the authors and does not necessarily represent the official views of the National Institutes of Health. AYR was partially supported by the Gerstacker fellowship program, the University of Michigan Rackham Merit Fellowship program, and the NIH Training Program in Translational Cardiovascular Research and Entrepreneurship (T32-HL125242).

References

1. Peripheral Arterial Disease in People With Diabetes. Diabetes Care. 2003; 26:3333–41. [PubMed: 14633825]
2. Varu VN, Hogg ME, Kibbe MR. Critical limb ischemia. Journal of vascular surgery. 2010; 51:230–41. [PubMed: 20117502]
3. Falluji N, Mukherjee D. Critical and acute limb ischemia: an overview. Angiology. 2014; 65:137–46. [PubMed: 23277633]
4. Leaper DJ. Silver dressings: their role in wound management. International wound journal. 2006; 3:282–94. [PubMed: 17199764]
5. Kirsner RS, Sabolinski ML, Parsons NB, Skornicki M, Marston WA. Comparative effectiveness of a bioengineered living cellular construct vs. a dehydrated human amniotic membrane allograft for the treatment of diabetic foot ulcers in a real world setting. Wound Repair and Regeneration. 2015; 23:737–44. [PubMed: 26100572]
6. Galiano RD, Tepper OM, Pelo CR, Bhatt KA, Callaghan M, Bastidas NN, Bunting S, Steinmetz HG, Gurtner GC. Topical Vascular Endothelial Growth Factor Accelerates Diabetic Wound Healing through Increased Angiogenesis and by Mobilizing and Recruiting Bone Marrow-Derived Cells. The American Journal of Pathology. 2004; 164:1935–47. [PubMed: 15161630]
7. Nichol JW, Khademhosseini A. Modular Tissue Engineering: Engineering Biological Tissues from the Bottom Up. Soft matter. 2009; 5:1312–9. [PubMed: 20179781]
8. Dean DM, Napolitano AP, Youssef J, Morgan JR. Rods, tori, and honeycombs: the directed self-assembly of microtissues with prescribed microscale geometries. Faseb J. 2007; 21:4005–12. [PubMed: 17627028]
9. Dean DM, Morgan JR. Cytoskeletal-mediated tension modulates the directed self-assembly of microtissues. Tissue engineering Part A. 2008; 14:1989–97. [PubMed: 18673088]
10. Dean DM, Rago AP, Morgan JR. Fibroblast elongation and dendritic extensions in constrained versus unconstrained microtissues. Cell motility and the cytoskeleton. 2009; 66:129–41. [PubMed: 19170224]
11. Kelm JM, Djonov V, Ittner LM, Fluri D, Born W, Hoerstrup SP, Fussenegger M. Design of custom-shaped vascularized tissues using microtissue spheroids as minimal building units. Tissue engineering. 2006; 12:2151–60. [PubMed: 16968156]
12. McGuigan AP, Sefton MV. Vascularized organoid engineered by modular assembly enables blood perfusion. Proceedings of the National Academy of Sciences of the United States of America. 2006; 103:11461–6. [PubMed: 16864785]
13. Youssef J, Nurse AK, Freund LB, Morgan JR. Quantification of the forces driving self-assembly of three-dimensional microtissues. Proceedings of the National Academy of Sciences of the United States of America. 2011; 108:6993–8. [PubMed: 21482784]

14. Gupta R, Sefton MV. Application of an endothelialized modular construct for islet transplantation in syngeneic and allogeneic immunosuppressed rat models. Tissue engineering Part A. 2011; 17:2005–15. [PubMed: 21449709]
15. Cheng HW, Luk KD, Cheung KM, Chan BP. In vitro generation of an osteochondral interface from mesenchymal stem cell-collagen microspheres. Biomaterials. 2011; 32:1526–35. [PubMed: 21093047]
16. Wang L, Rao RR, Stegemann JP. Delivery of mesenchymal stem cells in chitosan/collagen microbeads for orthopedic tissue repair. Cells, tissues, organs. 2013; 197:333–43. [PubMed: 23571151]
17. Wise JK, Alford AI, Goldstein SA, Stegemann JP. Comparison of uncultured marrow mononuclear cells and culture-expanded mesenchymal stem cells in 3D collagen-chitosan microbeads for orthopedic tissue engineering. Tissue engineering Part A. 2014; 20:210–24. [PubMed: 23879621]
18. Leung BM, Miyagi Y, Li RK, Sefton MV. Fate of modular cardiac tissue constructs in a syngeneic rat model. Journal of tissue engineering and regenerative medicine. 2013
19. Futrega K, P J, Kinney M, Lott WB, Ungrin MD, Zandstra PW, Doran MR. The microwell-mesh: a novel device and protocol for the high throughput manufacturing of cartilage microtissues. Biomaterials. 2015
20. Yen C-M, Chan C-C, Lin S-J. High-throughput reconstitution of epithelial–mesenchymal interaction in folliculoid microtissues by biomaterial-facilitated self-assembly of dissociated heterotypic adult cells. Biomaterials. 2010; 31:4341–52. [PubMed: 20206989]
21. Daley EL, Coleman RM, Stegemann JP. Biomimetic microbeads containing a chondroitin sulfate/chitosan polyelectrolyte complex for cell-based cartilage therapy. Journal of materials chemistry B, Materials for biology and medicine. 2015; 3:7920–9.
22. Rowe SL, Stegemann JP. Microstructure and Mechanics of Collagen-Fibrin Matrices Polymerized Using Ancrod Snake Venom Enzyme. J Biomech Eng-T Asme. 2009; 131
23. Ghajar CM, Chen X, Harris JW, Suresh V, Hughes CC, Jeon NL, Putnam AJ, George SC. The effect of matrix density on the regulation of 3-D capillary morphogenesis. Biophysical journal. 2008; 94:1930–41. [PubMed: 17993494]
24. Rao RR, Peterson AW, Ceccarelli J, Putnam AJ, Stegemann JP. Matrix composition regulates three-dimensional network formation by endothelial cells and mesenchymal stem cells in collagen/fibrin materials. Angiogenesis. 2012; 15:253–64. [PubMed: 22382584]
25. Rioja AY, Tiruvannamalai Annamalai R, Paris S, Putnam AJ, Stegemann JP. Endothelial sprouting and network formation in collagen- and fibrin-based modular microbeads. Acta biomaterialia. 2016; 29:33–41. [PubMed: 26481042]
26. Peterson AW, Caldwell DJ, Rioja AY, Rao RR, Putnam AJ, Stegemann JP. Vasculogenesis and angiogenesis in modular collagen-fibrin microtissues. Biomater Sci-Uk. 2014; 2:1497–508.
27. Kirkpatrick CJ, Fuchs S, Unger RE. Co-culture systems for vascularization—learning from nature. Adv Drug Deliv Rev. 2011; 63:291–9. [PubMed: 21281686]
28. Au P, Daheron LM, Duda DG, Cohen KS, Tyrrell JA, Lanning RM, Fukumura D, Scadden DT, Jain RK. Differential in vivo potential of endothelial progenitor cells from human umbilical cord blood and adult peripheral blood to form functional long-lasting vessels. Blood. 2008; 111:1302–5. [PubMed: 17993613]
29. Merfeld-Clauss S, Gollahalli N, March KL, Traktuev DO. Adipose tissue progenitor cells directly interact with endothelial cells to induce vascular network formation. Tissue engineering Part A. 2010; 16:2953–66. [PubMed: 20486792]
30. Shepherd BR, Jay SM, Saltzman WM, Tellides G, Pober JS. Human aortic smooth muscle cells promote arteriole formation by coengrafted endothelial cells. Tissue engineering Part A. 2009; 15:165–73. [PubMed: 18620481]
31. Nakatsu MN, Sainson RCA, Aoto JN, Taylor KL, Aitkenhead M, Pérez-del-Pulgar S, Carpenter PM, Hughes CC. Angiogenic sprouting and capillary lumen formation modeled by human umbilical vein endothelial cells (HUVEC) in fibrin gels: the role of fibroblasts and Angiopoietin-1☆. Microvascular Research. 2003; 66:102–12. [PubMed: 12935768]
32. Montesano R, Pepper MS, Orci L. Paracrine induction of angiogenesis in vitro by Swiss 3T3 fibroblasts. Journal of cell science. 1993; 105(Pt 4):1013–24. [PubMed: 7693734]

33. Thompson HG, Truong DT, Griffith CK, George SC. A three-dimensional in vitro model of angiogenesis in the airway mucosa. Pulmonary Pharmacology & Therapeutics. 2007; 20:141–8. [PubMed: 16414296]
34. Ghajar CM, Blevins KS, Hughes CC, George SC, Putnam AJ. Mesenchymal stem cells enhance angiogenesis in mechanically viable prevascularized tissues via early matrix metalloproteinase upregulation. Tissue engineering. 2006; 12:2875–88. [PubMed: 17518656]
35. Fernandez-Cossio S, Leon-Mateos A, Sampedro FG, Oreja MTC. Biocompatibility of agarose gel as a dermal filler: Histologic evaluation of subcutaneous implants. Plast Reconstr Surg. 2007; 120:1161–9. [PubMed: 17898590]
36. Bloch K, Vanichkin A, Damshkaln LG, Lozinsky VI, Vardi P. Vascularization of wide pore agarose-gelatin cryogel scaffolds implanted subcutaneously in diabetic and non-diabetic mice. Acta biomaterialia. 2010; 6:1200–5. [PubMed: 19703598]
37. Bhat S, Kumar A. Cell proliferation on three-dimensional chitosan-agarose-gelatin cryogel scaffolds for tissue engineering applications. Journal of bioscience and bioengineering. 2012; 114:663–70. [PubMed: 22884715]
38. Bhat S, Tripathi A, Kumar A. Supermacroprous chitosan-agarose-gelatin cryogels: in vitro characterization and in vivo assessment for cartilage tissue engineering. Journal of the Royal Society, Interface / the Royal Society. 2011; 8:540–54.
39. Yang Q, Zhang YY, Liu ML, Zhang YQ, Yao SZ. Study of fibrinogen adsorption on hydroxyapatite and TiO2 surfaces by electrochemical piezoelectric quartz crystal impedance and FTIR-ATR spectroscopy. Anal Chim Acta. 2007; 597:58–66. [PubMed: 17658313]
40. Lü XY, Yan H, Zheng BZ, Wu AP. Comparing adsorptive property of natural and synthesized hydroxyapatite to albumin, fibrinogen and IgG. Key Engineering Materials: Trans Tech Publ. 2007:869–72.
41. Yongli C, Xiufang Z, Yandao G, Nanming Z, Tingying Z, Xinqi S. Conformational Changes of Fibrinogen Adsorption onto Hydroxyapatite and Titanium Oxide Nanoparticles. Journal of colloid and interface science. 1999; 214:38–45. [PubMed: 10328894]
42. He J, Genetos DC, Leach JK. Osteogenesis and trophic factor secretion are influenced by the composition of hydroxyapatite/poly(lactide-co-glycolide) composite scaffolds. Tissue engineering Part A. 2010; 16:127–37. [PubMed: 19642853]
43. He J, Decaris ML, Leach JK. Bioceramic-mediated trophic factor secretion by mesenchymal stem cells enhances in vitro endothelial cell persistence and in vivo angiogenesis. Tissue engineering Part A. 2012; 18:1520–8. [PubMed: 22546052]
44. Mima Y, Fukumoto S, Koyama H, Okada M, Tanaka S, Shoji T, Emoto M, Furuzono T, Nishizawa Y, Inaba M. Enhancement of Cell-Based Therapeutic Angiogenesis Using a Novel Type of Injectable Scaffolds of Hydroxyapatite-Polymer Nanocomposite Microspheres. Plos One. 2012; 7
45. Becker JC, Domschke W, Pohle T. Biological in vitro effects of fibrin glue: fibroblast proliferation, expression and binding of growth factors. Scandinavian journal of gastroenterology. 2004; 39:927–32. [PubMed: 15513329]
46. Batorsky A, Liao J, Lund AW, Plopper GE, Stegemann JP. Encapsulation of adult human mesenchymal stem cells within collagen-agarose microenvironments. Biotechnology and bioengineering. 2005; 92:492–500. [PubMed: 16080186]
47. Carpentier G. ImageJ contribution: Angiogenesis Analyzer. ImageJ News. 2012
48. Hauschka PV, Wians FH Jr. Osteocalcin-hydroxyapatite interaction in the extracellular organic matrix of bone. The Anatomical record. 1989; 224:180–8. [PubMed: 2549810]
49. Gailit J, Clarke C, Newman D, Tonnesen MG, Mosesson MW, Clark RA. Human fibroblasts bind directly to fibrinogen at RGD sites through integrin alpha(v)beta3. Experimental cell research. 1997; 232:118–26. [PubMed: 9141628]
50. Grumezescu, A. Applications of Nanobiomaterials. William Andrew; 2016. Nanobiomaterials in Galenic Formulations and Cosmetics.

Statement of Significance

Critical limb ischemia (CLI) is a chronic disease that can lead to tissue necrosis, amputation, and death. Cell-based therapies are being explored to restore blood flow and prevent the complications of CLI. In this study, we developed small, non-aggregating agarose-hydroxyapatite-fibrinogen microbeads that contained endothelial cells and fibroblasts. Microbeads were easy to handle and culture, and endothelial sprouts formed within and between microbeads. Our data demonstrates that the composition of the microbead matrix altered the degree of endothelial sprouting, and that the addition of hydroxyapatite and fibrinogen resulted in more distributed sprouting compared to pure fibrin microbeads. The microbead format and control of the matrix formulation may therefore be useful in developing revascularization strategies for the treatment of ischemic disease.

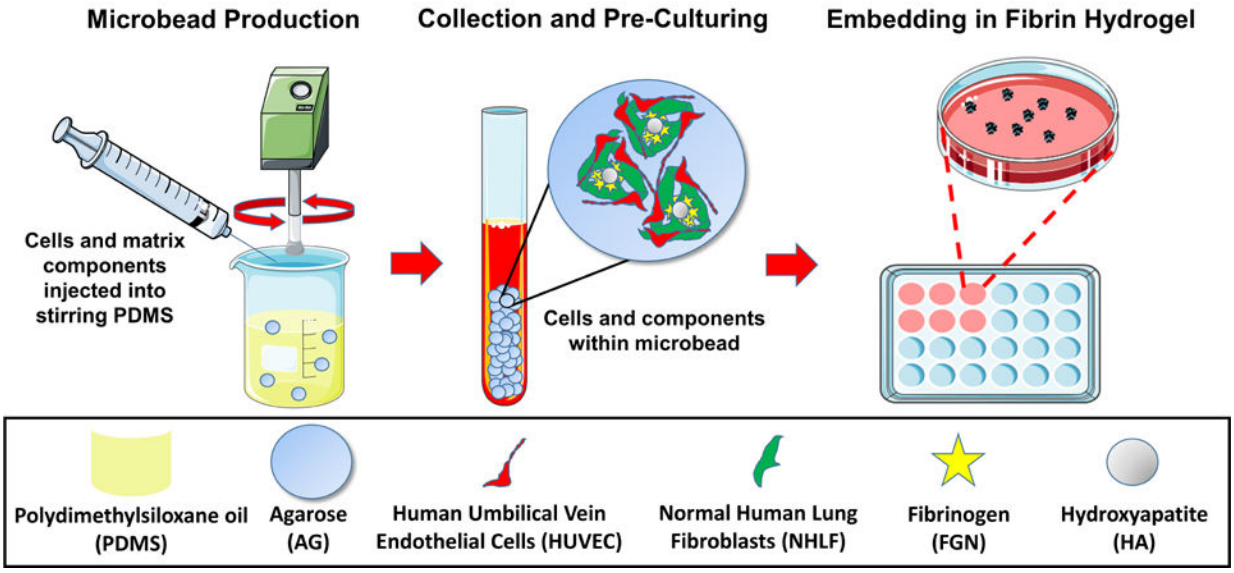

Figure 1. Microbead production and culturing

Agarose-based, cell-encapsulating microbeads were produced using a water-in-oil emulsion process. HUVEC and NHLF were incorporated in a 1:1 ratio at 2×10^6 total cells per mL of aqueous microbead components. Microbeads were pre-cultured for Days 1 and/or 7 and then embedded in fibrin hydrogels. Some images were adapted from Servier Medical Arts clipart (www.servier.com).

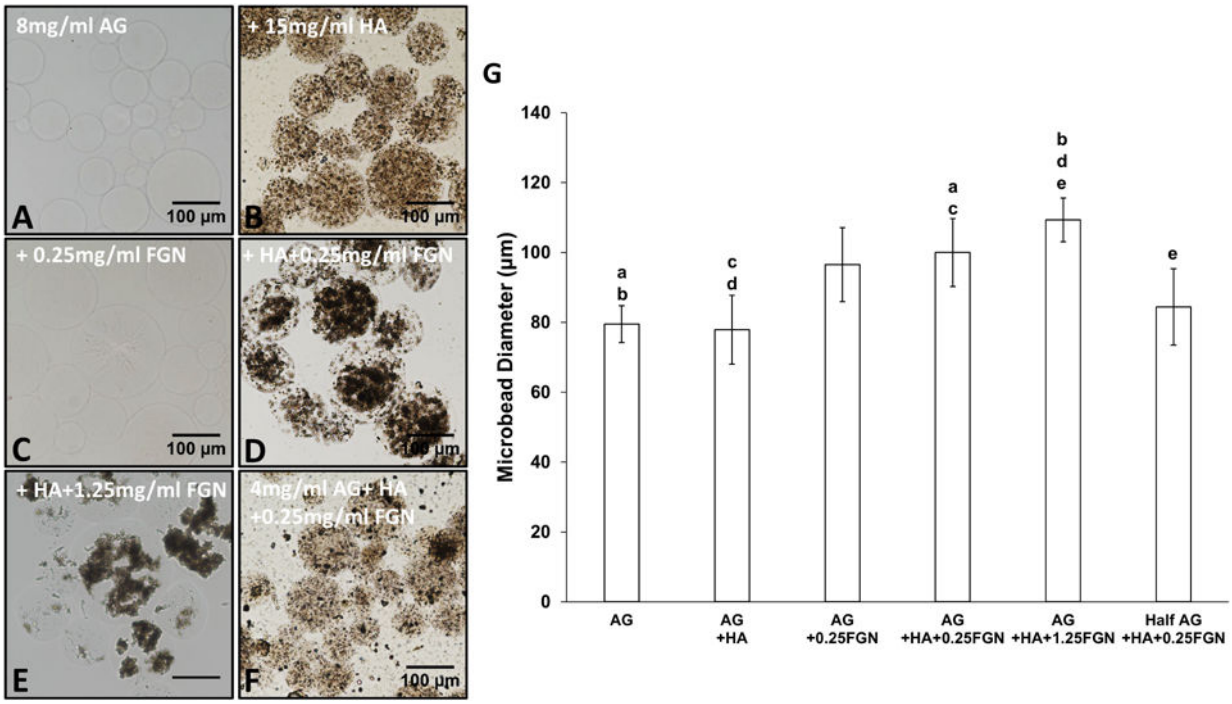

Figure 2. Microbead formulation characterization

Bright-field images showing incorporation of varying concentrations of FGN and HA into AG-based microbeads: (A) AG only microbeads and those made from 8 mg/mL AG + (B)HA, (C)FGN, (D)HA+ FGN, (E) 15 mg/mL HA+1.25 mg/mL FGN and (F) 4 mg/mL AG +15 mg/mL HA+0.25 mg/mL FGN. (G) Microbead size quantification. Lowercase letters indicate comparisons for which $p \leq 0.05$ (one-way ANOVA).

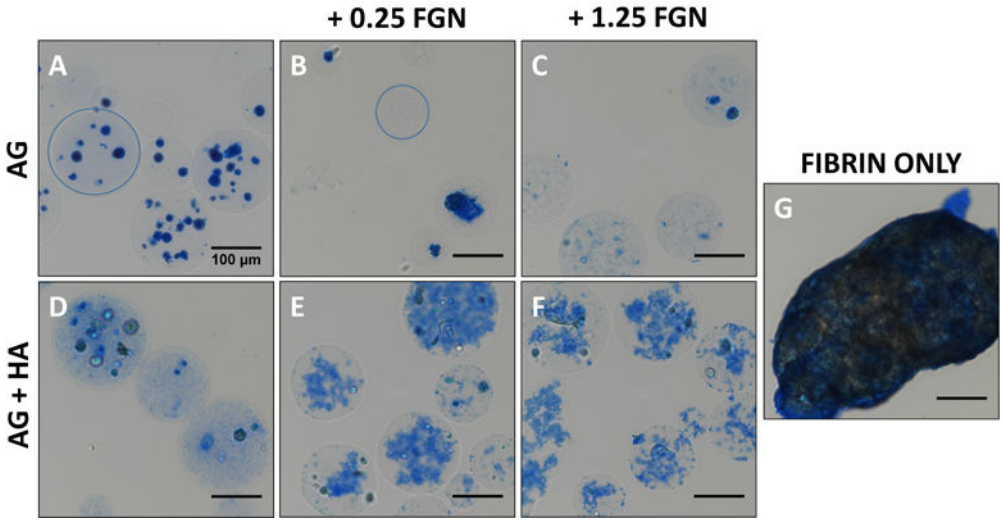

Figure 3. Greater concentrations of FGN permit the formation of homogenous, non-adherent HUVEC-NHLF microbeads

(A) AG, (B) AG+0.25FGN, (C) AG+1.25FGN, (D) AG+HA, (E) AG+HA+0.25FGN, (F) AG+HA+1.25FGN, and (G) fibrin microbeads stained using EZ blue to visualize microbead protein content after processing. Microbead boundary indicated with blue circle. Scalebar = 100 μm.

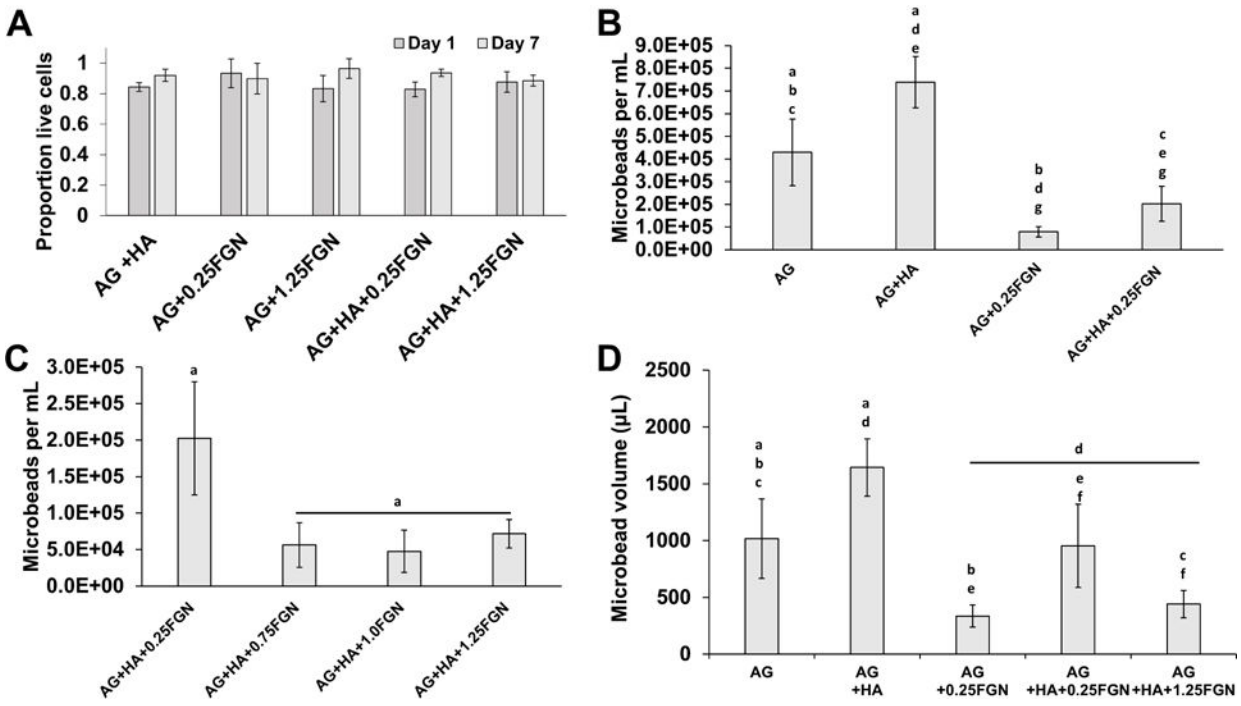

Figure 4. Effects of the different components on microbead yield and HUVEC-NHLF viability

(A) HA or FGN content had no significant effect on the viability of encapsulated cells one day after microbead production and after pre-culture. (B,C) Microbead yield increase with the addition of HA and decreased with the addition of FGN, until it reached steady-state at 0.75FGN. (D) Microbead volume based on microbead yield and microbead diameter. (Lowercase letters indicate comparisons for which $p \leq 0.05$ (one-way ANOVA).

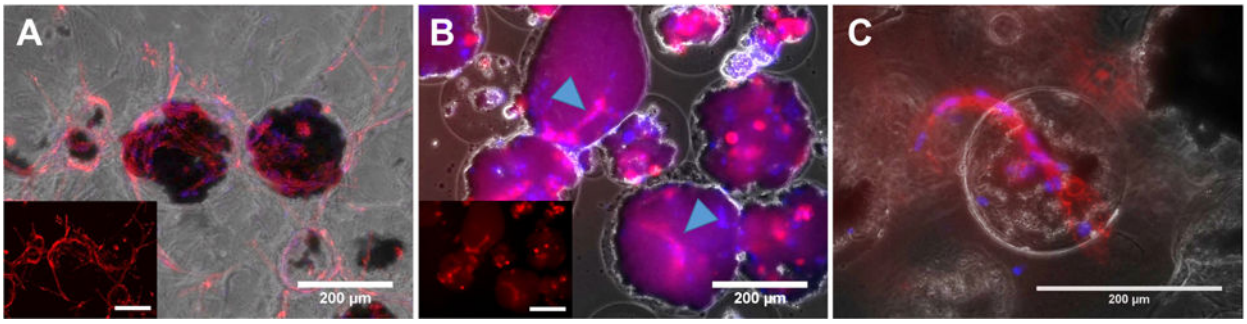

Figure 5. Proof of concept EC sprouting from Ag+15 mg/mL HA+0.25 mg/mL FGN microbeads under different culture conditions

(A) After 7 days of embedding in 2.5mg/mL FIB hydrogel (no pre-culturing). (B) After 7 days sedimentation in conical tube (no FIB embedding). Arrowheads indicate sprouts forming within microbeads. (C) After 5 days in FIB following 8 days pre-culturing in conical tube. Sprouts originated in the HA-FGN complex (black) located within the microbead boundaries (not visible). The inset in image A and B show endothelial cells stained in red. Red = UEA staining, Blue =DAPI. Scale bar = 200 μm.

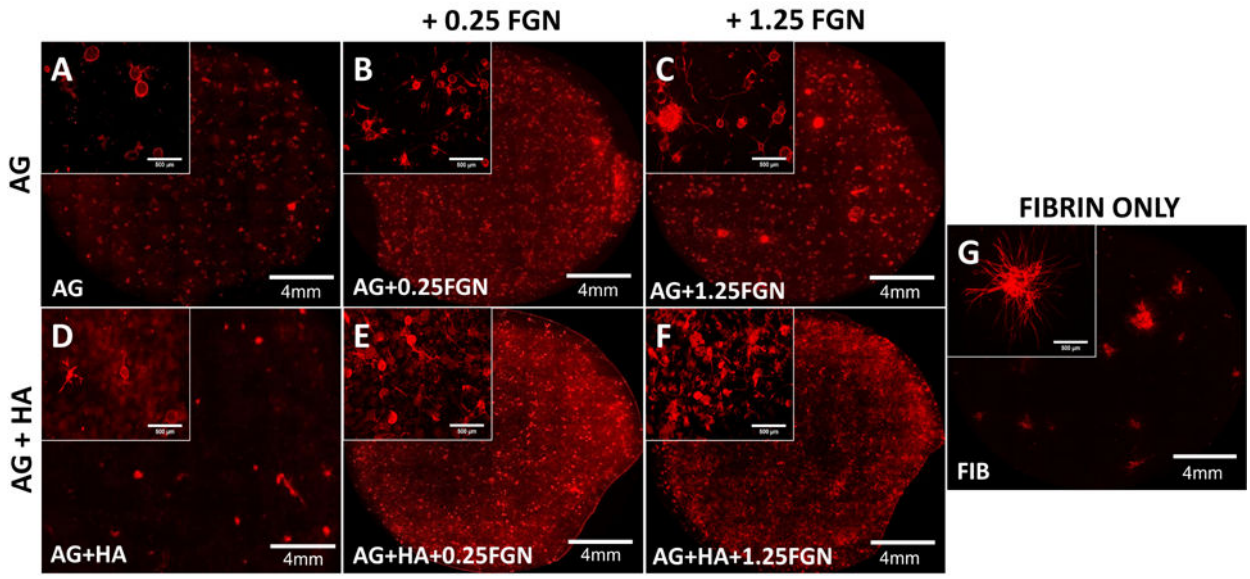

Figure 6. The distribution of HUVEC sprouting depends on microbead matrix components

(A) AG+HA, (B) AG+0.25FGN, (C) AG+1.25FGN, (D) FIBRIN, (E) AG+HA+0.25FGN, (F) AG+HA+1.25FGN microbeads were embedded in 2.5mg/mL FIB hydrogels and cultured for 7 days.

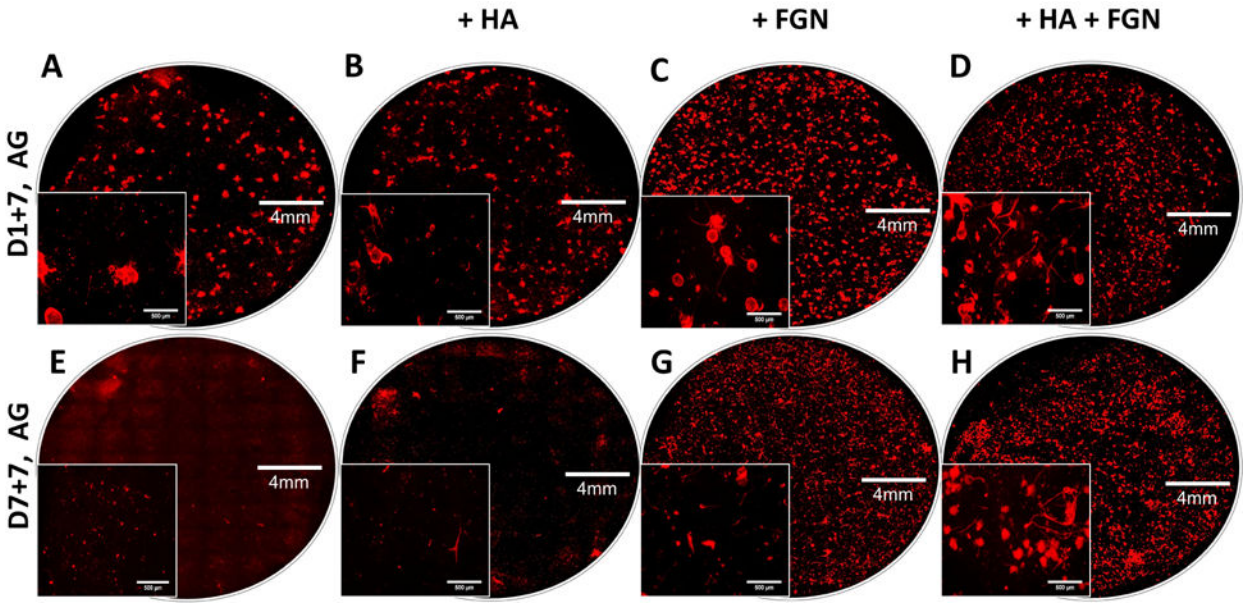

Figure 7. Fluorescence imaging reveals that HUVEC sprouting is affected by microbead composition and pre-culture conditions

Images of endothelial sprouting (red) from AG (A,E), AG+7.5HA (B,F), AG+1.25FGN (C,G), and AG+7.5HA+1.25FGN microbeads (D,H) embedded in fibrin hydrogels for 1 week; with (E,F,G,H), and without pre-culturing (A,B,C,D).

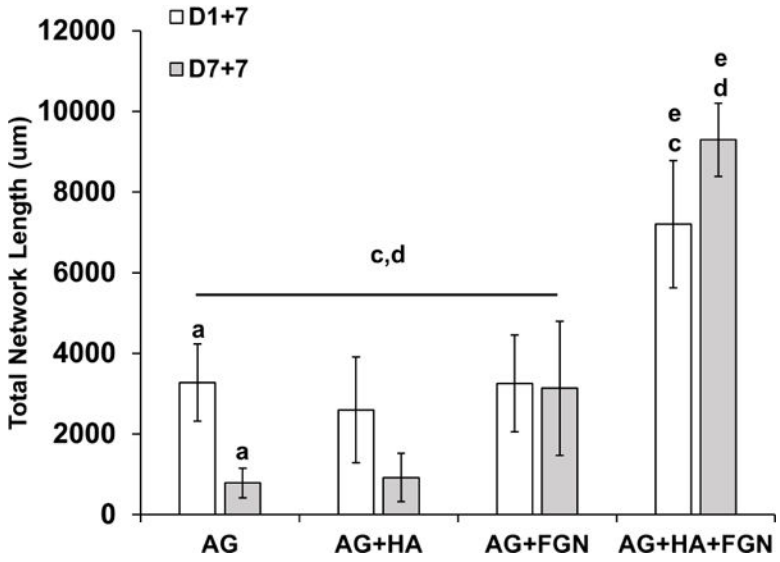

Figure 8. Quantification of total network length confirms that HUVEC sprouting is affected by microbead composition and pre-culture conditions

Quantification of microbeads, with/without pre-culturing, embedded in fibrin hydrogels for 1 week. Endothelial network length increased significantly when cells were encapsulated with HA and FGN in AG microbeads. Pre-culturing had a positive effect on total network length in AG+HA+FGN microbeads only. (Lowercase letters indicate comparisons for which $p \leq 0.05$ (one-way ANOVA).